Chapter 5. Diffusion in Solids

5.1 General features of diffusion

Solid-state diffusion is based on the ensemble of mechanisms by which atoms and point defects migrate through a crystal lattice. Diffusion is often the step that limits the rate of a process in a solid.

In this chapter, both the *microscopic* and *macroscopic* aspects of diffusion are reviewed. The former is useful in understanding the physics of migration and the origin of the material property called the *diffusivity* or the *diffusion coefficient* that quantifies the process. The latter is essential to calculating the concentration distribution of the diffusing species, the diffusion rate and the effect of irradiation on these properties.

The flow of solute atoms is called a *flux*, although strictly speaking, it is a *current*. In either terminology, it represents the net number of atoms that pass a plane of unit area per unit time. The flux of solute atoms is driven by a chemical potential gradient, generically referred to as a force. The most common driving force is a non-uniform distribution of solute atoms, otherwise known as a concentration gradient. Other forces can result in movement of solute atoms relative to the host crystal, including a temperature gradient and an electric-field gradient.

We concentrate primarily on diffusion generated by a concentration gradient, referred to as *ordinary*, or *molecular* diffusion. Diffusion can occur in one, two or three dimensions. The most common is three-dimensional diffusion, in which the diffusing species moves relative to the host lattice in any of the three directions. However, in anisotropic crystals, the diffusivities may not be equal. For example, in the hcp crystal structure (Fig. 3.8), the rate of movement in the **c** direction is different from the probability of migrating in the **a** directions.

Two-dimensional diffusion occurs on the surfaces of solids or along internal surfaces that separate the grains of polycrystalline solids. The latter is termed *grain boundary diffusion.* Movement of a trapped foreign atom along a dislocation line is an example of one-dimensional diffusion. In addition, macroscopic diffusion may appear to take place in fewer dimensions than that of the physical medium. For example, diffusion in a sphere with solute uniformly spread on the surface is a one-dimensional (radial) problem even though the sphere is a three dimensional body.

5.1.1 Diffusion in Nuclear Processes

Solid-state diffusion controls the rate of many important chemical and physical processes that take place in a nuclear fuel rod, a few of which are summarized in Table 5.1.

In the fast-neutron and fission-fragment fields inside a reactor core, many diffusion processes are accelerated. Atom mobility enhancement results from the point defects created in copious quantities by collisions of the energetic particles with the host atoms. In addition the motion of point defects proper is responsible for their agglomeration into *extended defects*, such as vacancies into voids and self-interstitials into disks. Consequently, it is important to keep track of

both the migrating species and the extended defects that result from the irradiation and diffusion processes.

Extended defects can profoundly affect the mechanical and dimensional properties of the structural metals and ceramics in which they form. Self-interstitial diffusion combined with the preferred orientation (texture) of Zircaloy produces the phenomena of preferred-direction growth (in the absence of stress) and irradiation creep (with stress present).

Process	Diffusing Species	Host Solid
Corrosion of cladding: - By water (normal operation) - By steam (severe accident)	 O^{2-} O	 ZrO_2 Zr
Hydriding of cladding	H	Zr
Fission gas release from fuel or bubble formation in fuel	Xe, Kr	UO_2
Sintering and creep of fuel	U^{4+}	UO_2

Table 5.1 Solid-State Diffusion Processes in Nuclear Materials

5.1.2 Types of diffusion coefficients

Diffusion processes are characterized by the identity of the moving species and path through the crystal (the mechanism) by which it moves. Below are several typical examples.

Self-diffusion characterizes the movement of a species in the absence of a concentration gradient. It refers to random motion of atoms or point defects in a solid. This is the type of diffusivity deduced from the atomic mechanisms discussed in Sect. 5.4. The measurement of a diffusion coefficient requires that a migrating species be identified. Thus, when similar atoms move, their motion is not detectable, so that strictly speaking there is no direct method for measuring the self-diffusion coefficient. However, if it is known for example that defect motion occurs by a vacancy mechanism, the motion of the vacancy can be measured, providing an indirect measure of the self-diffusion coefficient .

Tracer diffusion describes the mixing of different isotopes of the same element. It is the principal means of measuring self-diffusion coefficients. This diffusivity is subject to the same conditions as the self-diffusion coefficient except that some of the atoms are radioactive isotopes of the host element or ion. Measurement of the tracer diffusivity requires a gradient (and hence a flux) of the tracer but there is no gradient or flux of the combined radioactive and nonradioactive element or ion. Self-diffusivity and tracer-diffusivity are essentially equal.

Mutual diffusion and *chemical diffusion* are terms describing interchange of species A and B by diffusion. In binary solids, this diffusion coefficient, D_{AB} is related to the self-diffusion coefficients D_A and D_B by *Darken's equation* (Appendix A):

$$D_{AB} = (x_A D_B + x_B D_B)\left(\frac{\partial \ln a_A}{\partial \ln x_A}\right) \quad (5.1)$$

where a_A and x_A are the activity and mole fraction of component A, respectively. From the thermodynamics of the solution, a_A is a function of temperature and composition. In an *ideal solution*, $a_A = x_A$. The self-diffusivities D_A and D_B are functions of composition. In the second parenthetical term on the right, A can be replaced by B because the activities the two species are coupled (Prob. 5.3).

In addition to binary alloys, Eq (5.1) applies, for example, to the interdiffusion of U and Pu in $(U,Pu)O_2$ in a concentration gradient of the two cations.

The diffusivities defined above suffice for binary liquid systems, because the medium has no structure. In crystalline solids, on the other hand, the atoms are located on specific *sites* which possess distinctive geometrical properties (see Chap. 3). In addition, as discussed in Chap. 4, atoms can be missing from some sites (vacancies) or occupy positions that are not regular sites (self-interstitial atoms, or SIAs). These are termed *point defects.*

Solid-state diffusion requires the presence of point defects, of which vacancies are the most common. These are characterized by a diffusion coefficient D_V that is different from the atom diffusivity . An example of the latter is diffusion of vacancies in an irradiated metal to voids (Chap. 19).

5.2 Macroscopic description of diffusion

Just as thermodynamics can be described either from a macroscopic, classical viewpoint or in a microscopic, statistical setting, so can the process of diffusion be viewed in either of these two ways. The macroscopic laws of diffusion are combinations of a species conservation equation with a mathematical specification of the flux of the solute relative to the host substance.

5.2.1 Species Conservation

Conservation of a species whose concentration is c moles per unit volume is shown in Fig. 5.1[1]. The diagram shows a volume element of unit area and thickness *dz* . The flux of

[1] To simplify the notation, the subscripts denoting species in an AB solid are omitted. Thus $\tilde{D}_{AB}$ is reduced to D, flux J means J_A or J_B and concentration c can be either c_A or c_B.

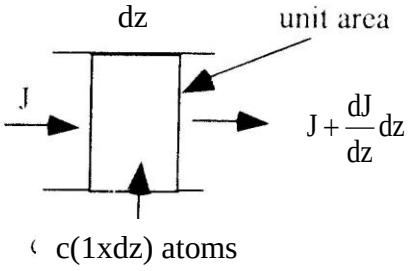

Fig. 5.1 Species conservation in a differential volume

diffusing species, J, is the number of atoms (or moles) crossing the unit plane per unit time. The plane is fixed relative to the crystal lattice. There may also be a source or sink of the species inside the volume element, *S*. The statement of species conservation is:

- time rate of change of moles of the species in the volume element = net influx of species + creation of the species in the volume element.

In mathematical terms, this word statement is:

$$\frac{\partial}{\partial t}(cdz) = J - \left(J + \frac{\partial J}{\partial z}dz\right) + Sdz$$

or

$$\frac{\partial c}{\partial t} = -\frac{\partial J}{\partial z} + S \qquad (5.2)$$

This conservation statement applies no matter what force is driving the flux J . Among the common forces are gradients of (i) the solute concentration; (ii) the temperature; (iii) the electric field. These lead, respectively, to fluxes describing ordinary molecular diffusion, thermal diffusion, and ionic transport. The electric field and ionic transport apply only to ceramics.

5.2.2 Fick's Laws of diffusion

When the concentration gradient drives J, the flux is given by *Fick's first law*:

$$J = -D\frac{\partial c}{\partial z} \qquad (5.3)$$

This equation follows the universal observation that matter moves from regions of high concentration to regions of low concentration, hence the minus sign. In principle the flux J and the concentration gradient are measurable quantities, so Eq (5.3) effectively defines the *diffusion coefficient* D. This definition of D is motivated by the fact that for small enough perturbation from equilibrium, i.e., for small enough concentration gradient, the flux is proportional to this driving force and D will be independent of the concentration gradient. In practice the value of D is approximately independent of the gradient for a wide range of gradient values. The units of D are length squared per unit time, (usually cm^2/s). J, c , and z must be in consistent units.

Substituting Eq (5.3) into Eq (5.2) gives *Fick's second law*:

$$\frac{\partial \mathrm{c}}{\partial \mathrm{t}} = \frac{\partial}{\partial \mathrm{z}}\left(\mathrm{D}\frac{\partial \mathrm{c}}{\partial \mathrm{z}}\right) + \mathrm{S} \tag{5.4}$$

This equation is also called the *diffusion equation*, by analogy to its heat transport counterpart, the heat conduction equation. In the common case of an isothermal system and D independent of solute concentration (and hence of z), and no source term, the diffusion equation simplifies to:

$$\frac{\partial c}{\partial t} = D\frac{\partial^2 c}{\partial z^2} \tag{5.5}$$

Analogous equations for cylindrical and spherical geometry involving one direction only, are:

Cylindrical geometry:

$$\frac{\partial c}{\partial t} = D\frac{1}{r}\frac{\partial}{\partial r}\left(r\frac{\partial c}{\partial r}\right) \tag{5.6}$$

Spherical geometry:

$$\frac{\partial c}{\partial t} = D\frac{1}{r^2}\frac{\partial}{\partial r}\left(r^2\frac{\partial c}{\partial r}\right) \tag{5.7}$$

5.3. Useful Analytical Solutions

There are a number of analytic solutions to the time-dependent, one-spatial-dimension diffusion equation. Compendiums of such solutions are contained in books by Carslaw and Jaeger [1] and Crank [2]. If the concentration is non-uniform in the directions transverse to z or r, additional second derivative terms are required on the right-hand sides of Eqs (5.5) – (5.7). However, mathematical solutions of multidirectional diffusion equations are considerably more complicated than those involving only one spatial dimension. Diffusion problems that are not amenable to closed-form solution can be solved by numerical techniques for which numerous computer codes are available.

5.3.1 Surface- source and diffusion-couple methods

Two common methods of measuring diffusivities in solids that are amenable to analytic solutions are depicted in Fig. 5.2. Sketch (a) shows the so-called *surface-source method*, in which a layer of pure solute (A) is deposited on a thick block of pure B into which A diffuses. The layer is assumed to be an inexhaustible source of in which component B is insoluble.

In Fig. 5.2 (b), the source of diffusing species is a block of pure A pressed firmly against a block of B containing an initial concentration c_o of A. This is termed a *diffusion couple*. In either

method the diffusing species can either be a different element from that which comprises the block on the right or an isotope of this element.

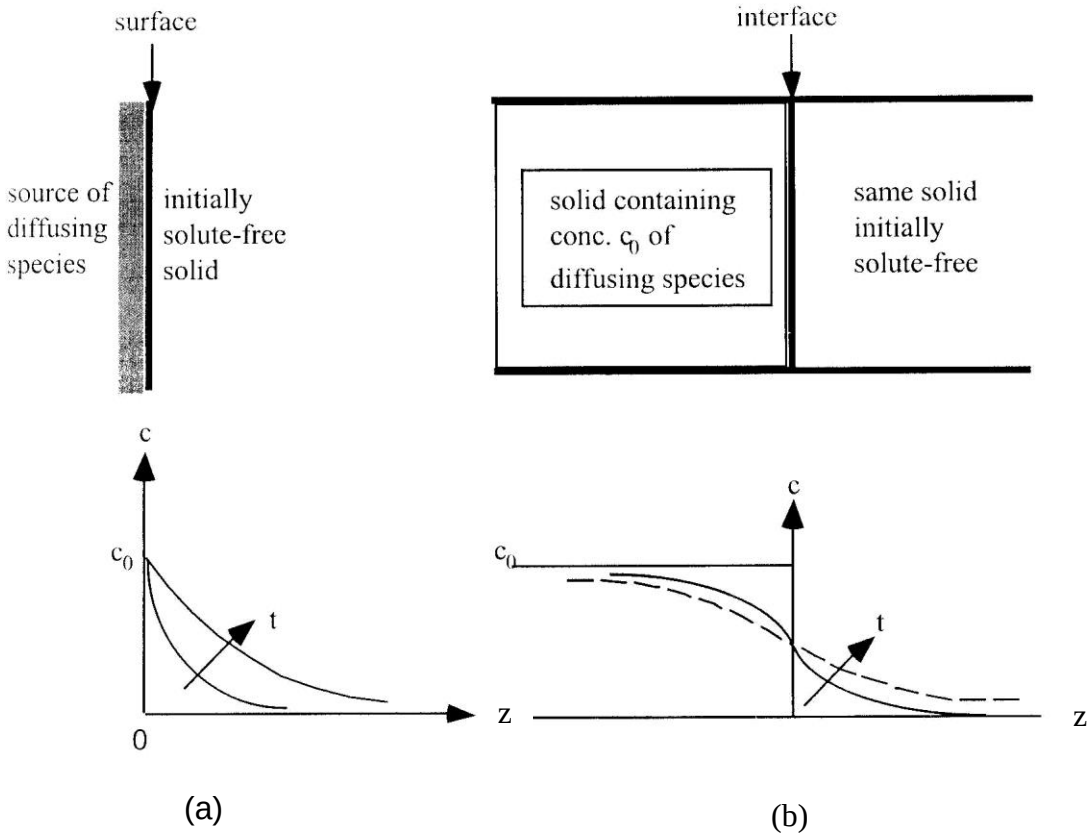

Fig. 5.2 Measurement of Diffusion Coefficients in Solids

The source of the diffusing solute need not be a layer of solid on the surface or another block containing the solute. It could equally well be a liquid or gas containing the solute that dissolves in the adjacent solid and provides the equilibrium concentration that drives the diffusion process.

The experiment is initiated by raising the temperature to a value at which the diffusivity is large enough to permit sufficient penetration of the solute into the initially solute-free zone for accurate measurement of the concentration to be made in a reasonable time. The diffusion equation is given by Eq (5.5) without the volumetric source term:

$$\frac{\partial c}{\partial t} = D\frac{\partial^2 c}{\partial z^2} \tag{5.8}$$

z extends from the surface or the interface into the initially solute-free blocks to the right in Fig. 5.2. The initial conditions for the two versions are identical:

$$c(z,0) = 0 \quad \text{for } z > 0 \tag{5.9}$$

The boundary conditions at z = 0 differ slightly:

$$\text{(source method)} \quad c(0,t) = c_0 \tag{5.10}$$

$$\text{(couple method)} \quad c(0,t) = c_0/2 \tag{5.11}$$

In the surface-source method, the surface layer produces an equilibrium concentration c_o in the adjacent block of B. This concentration remains constant until the layer A is completely depleted. Because of symmetry in the diffusion-couple technique, as soon as inter diffusion starts the concentration at the interface immediately becomes $c_o/2$ in both solids, and this value is retained throughout the diffusion anneal.

If the annealing time is sufficiently long, the diffusing solute reaches the far face of the initially pure-B block. However, for shorter times, this medium appears to be infinite in extent, and the boundary condition:

$$c(\infty,t) = 0 \tag{5.12}$$

applies to both versions of the experimental method.

Equations (5.8)- (5.12) are solved analytically by the similarity transform method given in Appendix B. The resulting solutions are:

Source method:
$$c(z,t) = c_o \operatorname{erfc}\left(\frac{z}{2\sqrt{Dt}}\right) \qquad 0 \le z \le \infty \tag{5.13}$$

Couple method:
$$c(z,t) = \frac{c_0}{2}\operatorname{erfc}\left(\frac{z}{2\sqrt{Dt}}\right) \qquad -\infty < z < \infty \tag{5.14}$$

The function erfc(ξ) of the dimensionless argument ξ is called the *complementary error function,* defined as erfc(ξ) = 1 – erf(ξ), where erf(ξ) is the tabulated *error function*:

$$erf(\xi) = \frac{2}{\sqrt{\pi}}\int_0^{\xi} \exp(-\xi'^2)\,d\xi' \tag{5.15}$$

The complementary error function erfc(ξ) is unity at ξ = 0 and decreases rapidly with increasing ξ. For example, erfc(2) = 0.0047. The evolution of the solute concentration distributions according to Eqs (5.13) and (5.14) are shown in the bottom of Fig. 5.2.

One method of determining D from such experiments is to slice thin layers of the initially solute-free blocks and measure the concentration of solute in each layer. Alternatively, the solids can be cut to obtain a cross section perpendicular to the surface or interface. The solute concentration profile is measured by one of a number of methods. For example, an energetic beam of highly collimated electrons or ions excites the solute species and radiation from decay of the excited

atoms is recorded by a suitable detector. The solute concentration profiles so obtained are fitted numerically to Eqs (5.13) or (5.14) to obtain the best-fitting value of D.

The arguments of the complementary error functions in Eqs (5.13) and (5.14)can be interpreted as the ratio of the variable depth z to a characteristic *diffusion depth*, $z_{diff} = 2\sqrt{Dt}$, or $\xi = z/z_{diff}$. The nature of the complementary error function is such that the penetration of solute is effectively limited to depths $z \leq \sim 2z_{diff}$ (where erfc = 0.0047). This condition serves to restrict the anneal time in the diffusion experiments when the thickness of the blocks of solid is a finite value L.

The methods described above are useful as long as the diffusivity is not dependent on composition, in which case the graphical methods described in Sect. 5.6 are employed.

Example #1 Diffusion penetration depth

If the solid blocks used in a diffusion couple experiment are 5 mm thick slabs and the diffusion coefficient of the solute is 10^{-10} cm^2/s, what is the maximum annealing time for which the boundary condition of Eq (5.12) is valid?

For the solute concentration to be essentially zero at the back face of the slab z = L, the time must be such that

$$L > 2\, z_{iff} = 4\sqrt{Dt_{max}}$$

Setting L = 0.5 cm and solving for the time gives $t_{max} = 1.6 \times 10^8$ s, which is > 5 years. The solute penetration depth for a more realistic experimental time of, say, 2 months (5×10^6 s) is

$$z_{diff} = 2\sqrt{10^{-10} \times 5 \times 10^6} = 0.045\,\text{cm}$$

or less than ½ mm. Sophisticated sampling methods are required in order to accurately measure a concentration distribution over such a small distance.

5.3.2 Instantaneous-Source Method

Instead of the inexhaustible surface source that led to the solution given by Eq (5.13), a common experimental technique involves depositing a thin layer of the diffusing species on the surface. This limited quantity is assumed to be immediately dissolved in a very thin layer of the large block. Equations (5.8), (5.9) and (5.12) apply to this so-called *instantaneous-source* situation, but Eq (5.10) is not valid at the surface. In its place, the quantity of diffusing species per cm^2 initially deposited on the surface (M) and subsequently completely diffused into the bulk is independent of time and must be conserved:

$$M = \int_0^\infty c(z,t)dz \qquad (5.16)$$

A solution of Eq (5.8) that satisfies the initial condition Eq (5.9) and the boundary condition Eq 2 is $c = Bt^{-1/2}\exp(-z^2/4Dt)$. B is a constant that is determined by substituting this solution into Eq (5.16) which yields $B = M/(\pi D)^{-1/2}$. The final solution for the concentration distribution is (Prob. 5.4):

$$c = \frac{M}{\sqrt{\pi Dt}} \exp\left(-\frac{z^2}{4Dt}\right) \qquad (5.17)$$

5.3.3 Diffusion in finite geometries

In this section, the geometries are a slab, a cylinder and a sphere. The diffusion equation must be solved by the method of separation of variables and the concentration distribution expressed as an infinite series instead of the closed form represented by the complementary error function for a thick slab.

The solutions for one-dimensional spherical, cylindrical, and slab geometries are given by Carslaw and Jaeger [1]. The equations solved are Eqs.(5.5), (5.6) and (5.7) without the source term. In slab geometry, the origin of z is the midplane, which permits the slab problem to be compared directly to the other two geometries. The initial condition are:

$$c(z,0) = 0 \qquad 0 < z < L, \qquad\qquad c(r,0) = 0 \qquad 0 < r < R \tag{5.18}$$

The boundary conditions at the surface are:

$$c(L,t) = c_o \qquad c(R,t) = c_o \tag{5.19a}$$

where L represents the half-thickness of the slab or the radius of a cylinder or sphere. Because of symmetry, the boundary condition at the origin is:

$$\left(\partial c / \partial z\right)_{z=0} = 0 \qquad\qquad \left(\partial c / \partial r\right)_{r=0} = 0 \tag{5.19b}$$

Figure 5.3 graphs the solutions of Eqs (5.5), (5.6) and (5.7) subject to the boundary conditions . Shown here is the volume average concentration $\bar{c}$ (relative to c_o) expressed in terms of the square root of the dimensionless time τ:

$$\tau = Dt / L^2 \quad \text{or} \quad Dt/R^2 \tag{5.19}$$

.

The analytic solution for the infinite medium can be regarded as a "short-time" approximation for the slab results in Fig. 5.7.

Example #2 Accuracy of the short-term solution

A 5 mm thick slab is exposed to a source of solute on its surface for 10^7 s. The diffusion coefficient is 10^{-9} cm^2/s. Compare the relative average concentration obtained from the analytical solution with that read from Fig. 5.3.

The dimensionless time is $Dt/L^2 = 10^{-9} \times 10^7/(0.5)^2 = 0.04$. The average concentration in the slab is M/L, where M_A, the total quantity of solute in the solid, is given by Eq (5.11):

$$\frac{\bar{c}}{c_o} = \frac{M/L}{c_o}\frac{2}{\sqrt{\pi}}\sqrt{\frac{Dt}{L^2}} = \frac{2}{\sqrt{\pi}}\sqrt{0.04} = 0.23$$

For comparison, on the curve for the slab in Fig. 5.3 for $\sqrt{Dt/L^2} = \sqrt{0.04} = 0.2$, $\bar{c}/c_o = 0.23$.

Although the two methods agree here, deviations begin at longer time.

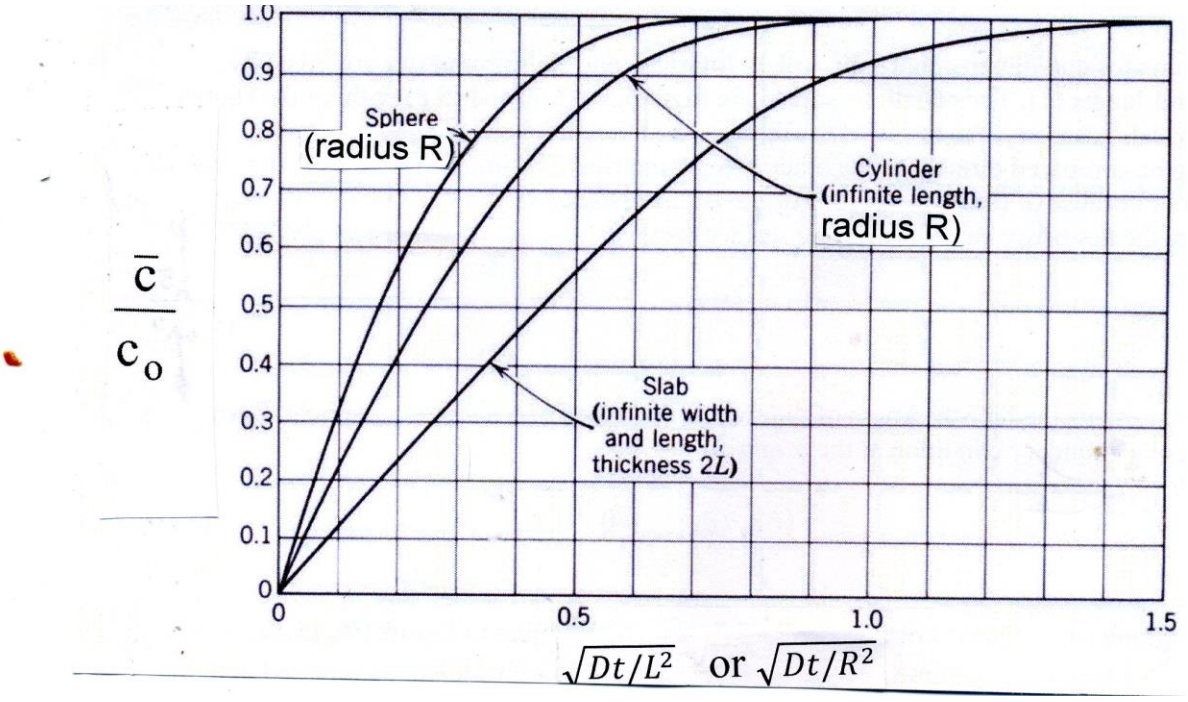

Fig. 5.3 Average solute concentration in a slab, cylinder, and sphere with zero initial concentration and a fixed concentration c_o at the surface (Ref. 1, p. 102)

5.3.4 Fission-Gas Release in Post-irradiation Annealing

The classical model of the release of the fission gases xenon and krypton is treated in Chap. 20. In this section, attention is restricted to the mathematical aspects of the theory as an example of the use of Fick's second law (the diffusion equation) in spherical coordinates. Briefly, the model assumes that the rate-limiting step is diffusion of the fission gases in the grains of uranium dioxide to the grain boundaries. The grains are modeled as spheres of radius R_{gr} . Upon reaching the periphery of the grains, the fission gas is assumed to be immediately released.

In a post-irradiation anneal experiment designed to measure the diffusivity of the fission gases, the UO_2 fuel specimen is irradiated in a neutron flux at a temperature sufficiently low that none of the fission gas is released. The irradiation produces a uniform concentration of Xe and Kr in the spherical grains representing the microstructure of the solid. The specimen is removed from the reactor and annealed at high temperature. Fission gas that escapes is trapped and measured by its radioactivity. This information yields the fraction of the fission gas released as a function of time, which is the quantity predicted by diffusion theory.

Assuming constant diffusivity, application of Eq (5.7), to this process givesi:

$$\frac{\partial c_{fg}}{\partial t} = D_{fg} \frac{1}{r^2} \frac{\partial}{\partial r}\left(r^2 \frac{\partial c_{fg}}{\partial r} \right) \tag{5.20}$$

with the initial condition:

$$c_{fg}(r,0) = c_{fgo} \tag{5.21}$$

and the boundary conditions:

$$\left(\frac{\partial c_{fg}}{\partial r}\right)_{r=0} = 0 \quad \text{and} \qquad c_{fg}(R_{gr},t) = 0 \tag{5.22}$$

where R_{gr} is the grain radius. The last of these boundary conditions arises from the assumption that the gas escapes without further resistance upon reaching the grain surface. The above analysis is referred to as the Booth model.

The "short-time" solution is developed by the Laplace transform method in Appendix C. The result for the average concentration in the sphere, or alternatively, the fraction of the initial amount released is:

$$f = 1 - \frac{\bar{c}_{fg}}{c_{fgo}} = 1 - \frac{6}{\sqrt{\pi}}\sqrt{\tau} + 3\tau \tag{5.23}$$

Where $\tau = D_{fg}\, t / R_{gr}^2$ is the dimensionless time. Equation (5.23) can be directly compared to the upper curve in Fig. 5.3, which is the exact solution. The comparison is direct because of the difference in the boundary and initial conditions used in the two methods; in Fig. 5.3, the initial condition is $c_{fg} = 0$ and the boundary condition at the periphery is $c_{fg} = c_{fgo}$. In the present solution, the initial and boundary conditions are reversed. Hence, the ordinate from Fig. 5.3 is to be compared to the fraction release from Eq (5.23).

Example: #3 fission-gas release
For $\tau = 0.1$, Eq (5.23) gives f = 0.23, .
From the upper curve of Fig. 5.3 at $\sqrt{\tau} = \sqrt{0.1} = 0.32$, read $f = 1 - \bar{c}_{fg} / c_{fg\,o} = 1 - 0.78 = 0.22$

Analytical solutions such as Eq (5.24) are useful for approximations to realistic diffusion situations. However, more complex boundary conditions, a time-dependent source term or concentration-dependent diffusivity need to be treated numerically (see Chap. 14).

5.4 Atomic Mechanisms of Diffusion in Solids

Although the previous sections provide a quantitative description of diffusion in solids, nothing is said about the mechanism . The mechanism (Fig. 5.4) was originally thought to be either (a) direct exchange an atom switches places with a nearest-neighbor or (b) a "ring" mechanism in which atoms execute coordinated jumps that produce the same result..

A distinction between self-diffusion of a host crystal and impurity diffusion in the host crystal is an important generalization. For most systems, self-diffusion is dominated by vacancies, since creating self-interstitials is usually a high-energy process. However,

impurities can be substitutional or interstitial, and both types of diffusion typically play a significant role.

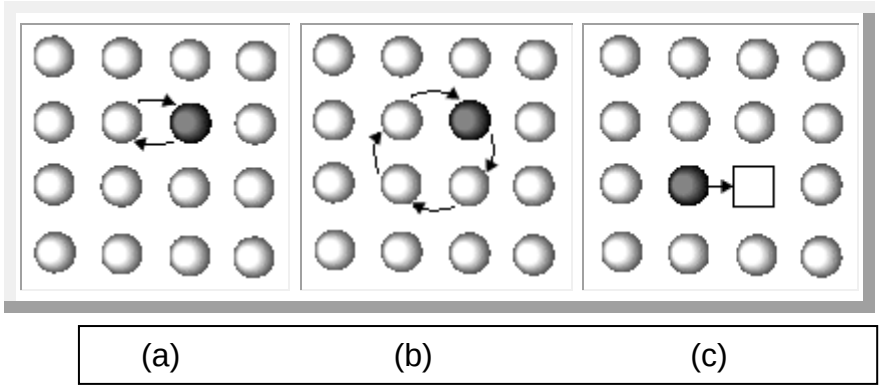

Fig. 5.4: The direct exchange (a), ring (b) and vacancy (c) diffusion mechanisms.

The operative mechanism (c) was demonstrated by Kirkendall in 1947 (ref. 4, p. 132) , which reported the results of the following clever experiment.

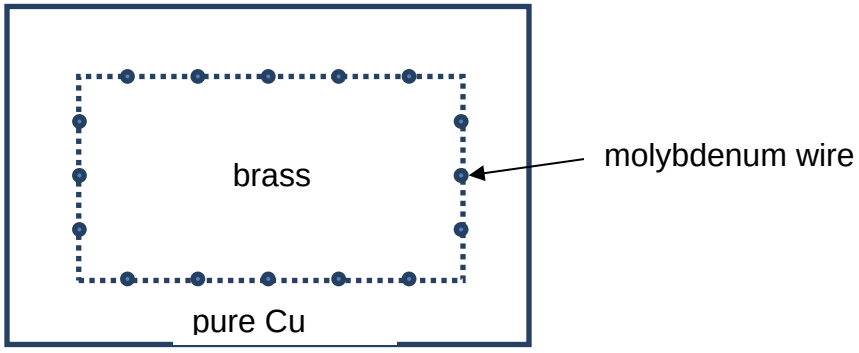

Figure 5.5: Schematic setup of Kirkendall's experiment [18]

In Fig. 5.5 a layer of Cu was electroplated around a bar of brass (70Cu30Zn alloy) on which molybdenum wires were laid down to serve as markers. The wires are inert as Mo neither dissolves in nor diffuses in the Cu/Zn alloy at the temperature of the experiment. This sample was then annealed at 1058 K for various times. The annealing results in interdiffusion of Cu and Zn. If diffusion involved an *exchange* or *ring* mechanism, the flux of Cu and Zn atoms across

the tungsten wire boundaries would balance and the distance between the tungsten wires would remain constant.

Instead, it was observed that the brass core *shrunk*, that is, the molybdenum wires got closer together as the annealing time increased. The interpretation was that the operative diffusion mechanism was (c) in Fig. 5.4, not (a) or (b). Because Zn diffuses outward faster than Cu diffuses inward, there is a net flow of Zn atoms out of the brass region, causing it to shrink. Simultaneously, there is a flux of vacancies in the opposite direction, which should have cancelled brass shrinkage due to loss of Zn. That this did not occur is due to the rapid re-establishment of the equilibrium vacancy concentration by removal of vacant lattice sites by filling with a metal atom. Had (a) or (b) been the driving mechanism, exchange of Cu and Zn atoms would not have caused movement of the Mo marker wires. This was the first demonstration that atomic diffusion in metals is mediated by point defects.

A vacancy flux caused by a chemical concentration gradient is called the Kirkendall effect. In Chapter 24 we will see how the *inverse* Kirkendall effect (chemical species flux resulting from a point-defect concentration gradient) can cause irradiation-induced segregation.

In general, diffusion of atomic species in metals depends on the presence of point defects which allow atomic motion to take place at the lowest energy. Movement of diffusing species (e.g., point defects, substitutional atoms, radioactively-tagged host atoms, interstitial impurities) relative to the host crystal ultimately depends upon the interatomic potential with which a solute atom interacts with surrounding host atoms and the analogous potential function between host atoms. These interatomic potentials are responsible for sites in the crystal lattice in which the potential energy of the diffusing species is a minimum. The migration process consists of movement of an atom between neighboring equilibrium sites, which requires passing through a potential energy barrier known as the *migration energy of diffusion* E_m.

The diffusion coefficient depends on:

- The lattice structure of the host crystal
- The equilibrium location of the diffusing species
- The path followed by the diffusing species through the lattice from one equilibrium site to another; the diffusion path will always be the one of least resistance, specifically the route that demands the lowest energy increase to effect the change in position.
- The temperature, which dictates the vibrational energy of all species in the system; the higher the temperature, the more likely is the diffusing species to acquire the necessary energy increment for migration.

5.4.1 Impurity motion between equilibrium sites

To illustrate the impurity-diffusion process, the elementary case of a small interstitial impurity atom migrating through a simple cubic lattice is shown in Fig. 5.6. The equilibrium site of the impurity atom is the center of the cube. At this position, the distance between the impurity atom and the nearest host atoms is the largest possible, which usually minimizes the repulsive potential interactions. Because of the thermal energy shared by all atoms of the system, the

impurity atom vibrates in three orthogonal [100] directions. The energy of each vibration is distributed according to a Boltzmann distribution, and very few of the vibrations possess sufficient energy to move to the adjacent
equilibrium site. The migration energy is the difference between the potential energy of the impurity atom at the midplane of its trajectory (the *barrier*) and the potential energy in

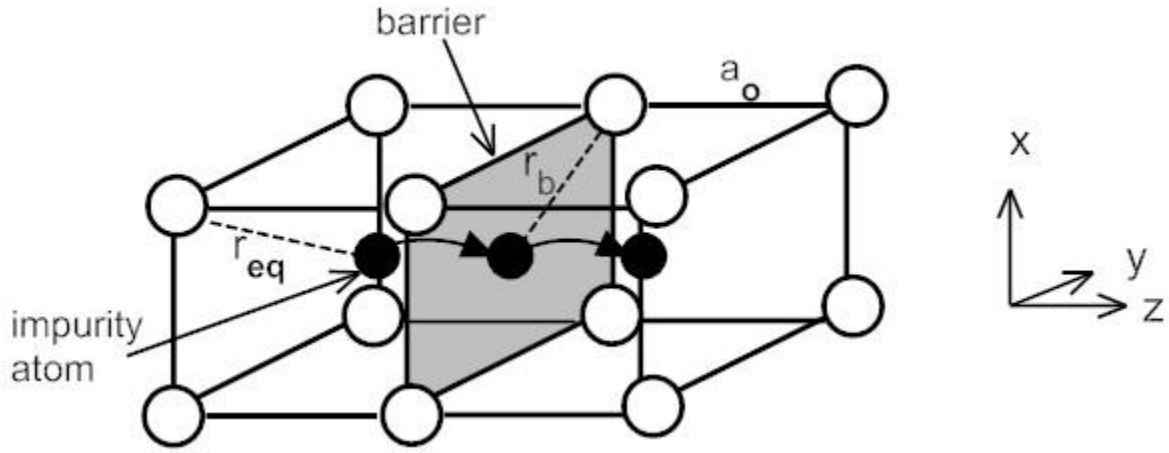

Fig. 5.6 Idealized jump of impurity atom in crystal with simple-cubic structure

the equilibrium site. The potential energy variation as the impurity atom moves along the jump direction is shown in Fig. 5.7. The dashed curves represent the components of the interatomic potential between the impurity atom and each of the host atoms in the diagram of Fig. 5.6. The energy in the equilibrium site, $U(r_{eq})$, is the sum of the potential energies of the pairwise interactions between the impurity atom and all of the neighboring host atoms. As the impurity atom moves along its path, its distance from the four atoms in the barrier plane is reduced to from r_{eq} to r_b, where the total energy is positive (repulsive). The sum of the interaction energies at this location is U_b, which is higher than U_{eq} by the barrier energy E_m . Only a very small fraction of the impurity atom vibrations in the equilibrium site have the requisite activation energy $E_{m.}$ to permit a jump. Because of the energy barrier, the diffusing species spends most of the time vibrating in equilibrium sites and only occasionally moves to an adjacent site. This movement is called a *jump*, the length of which is denoted by λ. For the diffusion mechanism illustrated in Fig. 5.6, the jump distance is one lattice parameter, a_o. For most realistic atomic mechanisms of diffusion, λ is smaller than a lattice parameter.

A parameter critical to quantitative description of the diffusion process on an atomic scale is the vibration frequency of the impurity atom in its equilibrium site, denoted by ν. In order to estimate ν, the potential energy curve U(r) at the equilibrium site in Fig. 5.7 is expanded in a two-term Taylor series about the equilibrium separation distance:

$$U(r) = U(r_{eq}) + \frac{1}{2}\left(\frac{dU^2}{d\,r^2}\right)_{r_{eq}} (r - r_{eq})^2 + \ldots \qquad (5.24)$$

The absence of the first derivative reflects the minimum of U at this location. The force on the vibrating impurity atom is the derivative of the potential energy:

$$F(r) = -\frac{dU}{d\,r} = -\left(\frac{dU^2}{d\,r^2}\right)_{r_{eq}} (r - r_{eq}) \tag{5.26}$$

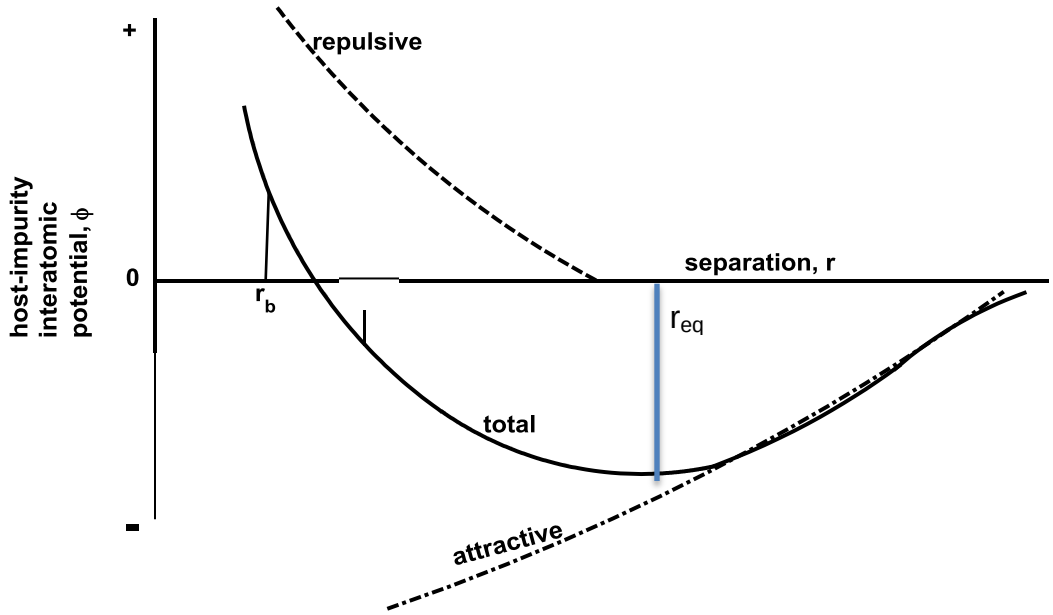

Fig. 5.7 Potential energy variation as the impurity atom moves along its migration path

This equation is formally identical to the restoring force on an extended spring, with the second derivative of U at r_{eq} serving as the spring constant. The linear restoring force leads to simple harmonic motion with an oscillation frequency:

$$\nu = \frac{1}{2\pi}\left[\frac{1}{m}\left(\frac{dU^2}{dr^2}\right)_{r_{eq}}\right]^{1/2} \tag{5.25}$$

where m is the mass of the impurity atom.

A reasonably accurate estimate of ν can be obtained by approximating the potential energy function ias a sinusoid of amplitude E_m and wavelength λ:

$$U(r) = U(r_{eq}) + E_m \sin^2\left(\frac{\pi(r - r_{eq})}{\lambda}\right) \tag{5.26}$$

Squaring the sine function has no other purpose than assuring positive U at all values of r. The second derivative of this function at r_{eq} is:

$$\left(\frac{dU^2}{dr^2}\right)_{r_{eq}} = \frac{2\pi^2}{\lambda^2} E_m \tag{5.27}$$

which, when substituted into Eq (5.28), yields:

$$\nu = \frac{1}{\sqrt{2}}\left[\frac{E_m}{m\lambda^2}\right]^{1/2} \tag{5.28}$$

Example #4a: Estimate the vibration frequency of the diffusing atom in its equilibrium position
In order to estimate ν, we take the mass of the diffusing atom to be that of hydrogen, a common impurity in many metals ($m = 10^{-3}$ kg/mole). In Fig 5.7 the jump distance is a lattice constant, or $\lambda \approx 3\text{x}10^{-10}$ m. There is no simple estimate of the barrier height E_m, theoretical knowledge of which would require a complete molecular model of the jump process (Chap. 14). Hence, we assume a typical value of 100 kJ/mole[2]. Using these values in Eq (5.28) yields the impurity atom vibration frequency:

$$\nu = \frac{1}{\sqrt{2}}\left(\frac{10^5\ \text{J/mole}}{10^{-3}\ \text{kg/mole} \times (3\times10^{-10})^2\ \text{m}^2}\right)^{1/2} \approx 2\times10^{13}\ \text{s}^{-1}$$

This computation makes use of the relationship for SI units J/kg = $(\text{m/s})^2$. The resulting vibration frequency is typical of atoms in a solid.

The frequency at which a diffusing atom succeeds in moving from an equilibrium site to an adjacent one is much less than its vibration frequency in the equilibrium site. The vast majority of the vibrations do not possess sufficient energy to overcome the energy barrier E_m The fraction with this energy is the Boltzmann factor $\exp(-E_m/R_gT)$. $R_g = 8.314$ J/mole-K is the gas constant and T is in Kelvins. The jump frequency (w) is thus:

$$w = \nu e^{-E_m/RT} \tag{5.29}$$

Example #4b: Estimate the jump frequency of an impurity atom at 1000 K with a barrier energy of 100 kJ/mole.

$$\text{w} = 2\text{x}10^{13} \exp\left(-\frac{96.5\text{x}10^3}{8.314\text{x}1000}\right) = 2\text{x}10^8\ \text{s}^{-1}$$

or, ten in a million vibrations result in a diffusional jump.

[2] E_m is commonly expressed in electron volts per atom (eV/atom).The conversion factor is 96.5 kJ/mole per eV/atom

The preceding explanation of the origin of Eq (5.29) is simple and leads to the approximately correct result. The rigorous derivation of this equation, however, is based on statistical mechanics and is considerably more complex than the "derivation" presented here (see Sect. 7.5 of Ref. 3).

5.4.2 The Einstein Equation

One of the most important equations in diffusion theory is attributed to Einstein. This equation connects the macroscopic property D, the diffusion coefficient, with the microscopic properties w, the jump frequency, and λ, and the jump distance, The original Einstein equation in three dimensions is presented in Sect. 7.3 of Ref. 3 and Sect. 2.3 of Ref. 4. Figure 5.8 is the basis of a simplified version in one dimension.

The diffusing atoms occupy interstitial planes at an areal density of n atoms per unit area, decreasing from left to right in the diagram. The jump distance λ is equal to a lattice constant, so the areal density n is related to the volumetric concentration c (atoms per unit volume) by $c = n/\lambda$. The rate of jumping from the left-hand plane of impurity atoms to the right-hand plane is

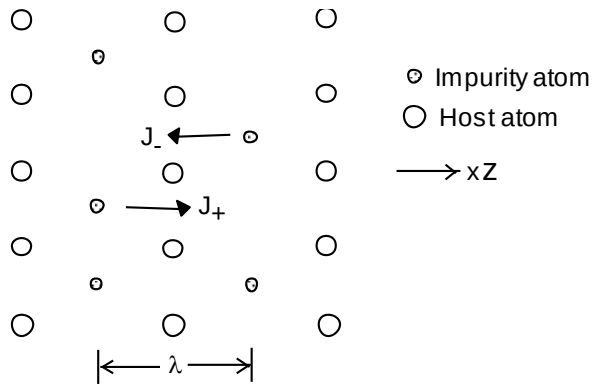

Fig. 5.8 One-dimensional diffusion

$J_+ = n(z)w$, where z is distance along the jump direction. In the opposite direction, the flux is $J_- = n(z+\lambda)w$. The net flux is:

$$J = J_+ - J_- = \big(n(z) - n(z+\lambda)\big)w = \lambda\big(c(z) - c(z+\lambda)\big)w \tag{5.30}$$

expanding $c(z+\lambda)$ in a one-term Taylor series, $c(z+\lambda) = c(z) + (\partial c/\partial z)\lambda$ converts the flux equation to:

$$J = -(\lambda^2 w)\frac{\partial c}{\partial z} \tag{5.31}$$

Comparison of this equation with the macroscopic definition of the diffusion coefficient given by Eq (5.3) shows that for this one-dimensional problem,

$$D_{1D} = \lambda^2 w \tag{5.32}$$

The quantity w is a one-way jump frequency, or the frequency with which an impurity atom jumps from an equilibrium site to a *particular* adjacent equilibrium site. The frequency with which the diffusing atom jumps to *any* available adjacent site is called the *total jump frequency*, and is denoted by Γ. In Fig. 5.8, only jumps to the left or the right are allowed, so Γ = 2w, and the above equation becomes:

$$D_{1D} = \tfrac{1}{2}\lambda^2\Gamma \tag{5.33}$$

In three-dimensions, ½ in the above equation is replaced by 1/6 and $\Gamma = \beta w$, where β is the number of sites that are within a jump's length of the diffusing atom:

$$D = \tfrac{1}{6}\lambda^2\Gamma = \tfrac{1}{6}\lambda^2\beta w \tag{5.34}$$

which is the *Einstein formula*. The value of β and the relation of λ to the lattice parameter depend on the crystal structure and the diffusion mechanism.

Example # 5 the Einstein formula in the simple-cubic lattice

In Fig. 5.6, $\lambda = a_o$, the lattice parameter, and β = 6, representing the six faces through which the impurity atom can jump into the six nearest equivalent jump sites. Using these values in Eq (5.34) and expressing w by Eq (5.29) gives:

$$D = \nu a_o^2 \exp(-E_m / RT) \tag{5.35}$$

Example # 6 the diffusion coefficient of an impurity atom in the bcc lattice.

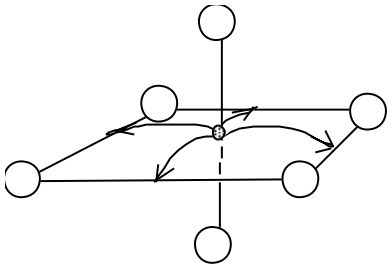

Fig. 5.9 Impurity-atom diffusion in the bcc lattice

Figure 5.9 shows a (100) plane of the bcc lattice (Fig. 3.5). Also indicated above and below the (100) plane are two body-centered atoms in adjacent unit cells.. The equilibrium site for the impurity atom is the octahedral site (the center of the (100) plane – see also Fig. 4.2). The edges of (100) plane are also octahedral interstitial sites. The impurity atom jumps are indicated by the four arrows. The jump distance

is $\lambda = 0.5a_o$ and the jump frequency multiple is $\beta = 4$. According to Eq (5.34), the diffusivity of the impurity atom is:

$$D = \frac{1}{6}(\frac{1}{2}a_o)^2(4w) = \frac{1}{6}a_o^2 \nu \exp\left(-\frac{E_m}{RT}\right) \tag{5.36}$$

5.4.3 The Vacancy Mechanism

In nearly all metals, self-diffusion of host atoms and migration of substitutional impurity atoms occur by the *vacancy mechanism* (see also Sect. 5.4). An atom (host or impurity) on a regular

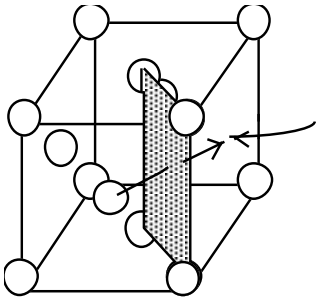

lattice site is surrounded by sites nearly all of which are oc
by exchanging places with an adjacent host atom because

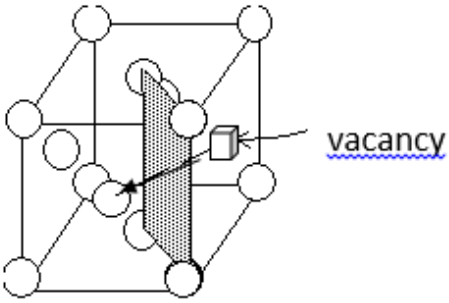

Fig. 5.10 fcc structure (a) atom jump into vacant lattic
lattice site

atom can move only if one of its nearest-neighbor sites is
mechanism operating in the fcc lattice The atom jump sho
vacancy jump in the opposite direction, which is depicted
two ways of portraying the same process. However, the end result depends on whether the diffusivity is considered to be that of the atom or the vacancy.

The barrier that controls the activation energy E_m is the shaded plane in the figure. In this location, the distance between the moving atom and the four corner atoms of the shaded plane is $r_b = \sqrt{3/8}\, a_o$, which is less than the separation of nearest neighbors in the equilibrium site, $r_{eq} = a_o / \sqrt{2}$. The energy barrier is due to the difference in these distances, as in Fig. 5.6.

We first consider the vacancy in Fig. 5.10b as the migrating species. In the fcc lattice, the jump distance is $a_o / \sqrt{2}$ and the number of allowable jump directions is $\beta = 12$. Using Eq (5.31) for the jump frequency in the Einstein formula of Eq (5.34), the vacancy diffusivity in the fcc crystal is:

$$D_v = a_o^2 \nu\, e \exp[-E_m / RT] \tag{5.37}$$

To analyze the atom migration process illustrated in Fig. 5.10a, the following difference between the movement of the two species must be recognized. For a vacancy jump, the

neighboring site must contain an atom. This probability is $1 - C_V^{eq}$, which is essentially unity because the vacancy fraction $C_V^{eq} << 1$ under all conditions. On the other hand for an atom to jump, a vacancy must occupy an adjacent site, the probability of which is C_V^{eq}. The requirement of an empty adjacent site is included in the Einstein formula as the equilibrium vacancy site fraction,

$$C_v^{eq} = exp(-E_f^v / RT) \tag{4.9a}$$

The relationship between the atom self-diffusion coefficient D and the vacancy diffusivity D_V is:

$$D = D_v C_v^{eq} \tag{5.38}$$

with D_V from Eq (5.37) and C_V^{eq} from Eq (4.9a), the atom diffusion coefficient is:

$$D = a_o^2 \, \nu \exp[-(E_m + E_f^v) / RT] \tag{5.39}$$

The addition of the energy of vacancy formation E_f^v to the energy of atom migration in the exponential accounts for the requirement of an adjacent vacancy to effect the atom jump.

Equation (5.40) does not apply to diffusion in an irradiation environment. Neutrons and fission-fragments create vacancies (and other defects) at a much higher rate than thermal processes. The resulting $C_V >> C_V^{eq}$ and the self-diffusity becomes

$$D = D_V C_V \tag{5.40a}$$

Although the interstitial variant of Eq (5.40) is negligible because C_I^{eq} is very small, irradiation can generate substantial self-interstitial concentrations. The self-diffusivity driven by interstitial motion:

$$D = D_{SIA} C_I \tag{5.40b}$$

can be larger than the vacancy-mediated D of Eq (5.40a).

The location of impurity atoms can be substitutional or interstitial, so diffusion of impurity atoms can be due to either a vacancy or an interstitial mechanism.

5.4.4 General diffusion formula

Independent of the mechanism responsible for the species' mobility, diffusion coefficients are often expressed as:

$$D = D_o \exp(-Q / RT) \tag{5.41a}$$

The pre-exponential factor D_o includes the jump distance and jump frequency and the activation energy Q accounts for the barrier height E_m and other energy requirements for atom movement, such as E_f^v in Eq (5.39).

5.5 Diffusion in Ionic Crystals

In a binary solid such as MX, vacancies (V) and interstitials (I) are present on both the cation (M) and anion (X) sublattices. The two types of diffusion coefficients required to characterize atomic motion are:

- Diffusivities of the point defects, D_{VX}, D_{IX}, D_{VM} and D_{IM}.
- Self-diffusion of the atomic species, D_X and D_M. These are closely linked to the point-defect diffusivities by the mechanism of atom movement. For example, if the cations move by a vacancy mechanism, there must be a vacancy next to an atom to enable jumping of the latter into a new position.

Diffusion in ionic crystals differs from that in metals and elements in numerous ways:

1. Ionic solids consist of at least two oppositely-charged components called cations (+) and anions (-) – see Sect.4.3.
2. Cations and anions generally exhibit very large differences in diffusivities; occasionally as large as seven orders of magnitude
3. The defect that predominates (Schottky or Frenkel) controls the magnitudes of the diffusivities via C^{eq} in Eq (5.40).
4. The effect of substitutional doping of ionic solids with cations of different valence from the host cation has a profound effect on the diffusivities.
5. The requirement of local electrical neutrality affects the movement of the ions.

On the other hand, there is considerable commonality between diffusion in metals and in ionic compounds:

1. The diffusion coefficients obey the Einstein equation, Eq (5.36)
2. The diffusion mechanisms commonly found in metals and elements (vacancy and interstitial mechanisms) also predominate in ionic solids
3. The various types of diffusion coefficients discussed in the preceding section (tracer, self, mutual) also characterize ionic solids.
4. Motion of the ions is restricted to the sublattice of the same charge. For an ionic solid with M = cation and X = anion, the self-diffusion coefficients are:

Vacancy mechanism:

$$D_M = D_{VM} C_{VM} \qquad \textit{and} \qquad D_X = D_{VX} C_{VX} \tag{5.40}$$

Interstitial mechanism:

$$D_M = D_{IM} C_{IM} \qquad \textit{and} \qquad D_X = D_{IX} C_{IX} \tag{5.41}$$

As in metals, the self-diffusion coefficients depend linearly on the site fractions of the point defect responsible for atom motion. These are the equilibrium values in a thermal environment or the much greater concentrations sustained by irradiation.
The diffusivities of the defects proper (D_{VM} …etc), are independent of their concentrations.

Not all four mechanisms are operative in a particular ionic solid. The mechanism that dominates for the cations may be different from that controlling anion motion.

In NaCl-type crystals (MX), the cation diffusivity is substantially larger than the anion diffusivity, or $D_M >> D_X$. In fluorite lattices MX_2, the opposite is true.

Example #7 Cation diffusivity in MX

The sketch below is one quarter of a full unit cell of the NaCl structure of Fig. 3.14 with a cation midway in its jump from site **a** along a face diagonal of the fcc sublattice into a nearest-neighbor cation vacancy at site **b**. The jump distance is one-half of the face diagonal of the full unit cell, or $\lambda = a_o / \sqrt{2}$ Since each cation vacancy in the fcc sublattice has 12 nearest neighbor cations, the jump-frequency multiple is $\beta = 12$. Substituting these factors into Eq (5.34) and using Eq (5.29), the cation vacancy diffusion coefficient is:

$$D_{VM} = a_o^2 \nu \exp\left(-E_m^{VM}/R_g T\right) \qquad (5.42)$$

(

where $a_o \sim 0.35$ nm is the lattice constant of the full NaCl unit cell i.e., the height of the two cubes in the sketch) and $\nu \sim 10^{13}$ s^{-1} is the vibration frequency of the cations.

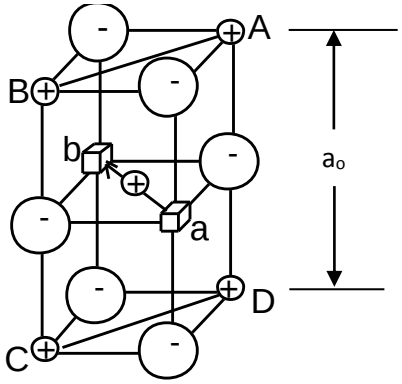

Fig. 5.11 Cation diffusivity in MX

At the midway position, the (110) plane ABCD is the barrier. Here, the Coulomb repulsion of the moving cation by the four corner cations is greater than the attraction of the two edge-centered anions. This net Coulomb repulsion is the source of the barrier energy E_m^{VM}, taken here to be 90 kJ/mole. The cation vacancy diffusivity at 1000 K from Eq (5.44) is $D_{VM} = 500$ nm^2/s (5×10^{-12} cm^2/s)

The diffusion coefficient of the cations is obtained by multiplying D_{VM} by the vacancy fraction, C_{VM}. For high-purity crystals, intrinsic point defects dominate and $C_{VM} = \sqrt{K_S}$, where K_S is the equilibrium constant for Schottky defects (method of Sect. 4.3.6 for MX). The activation energy for diffusion is the sum of the migration energy of the cation vacancy, E_m^{VM}, (assumed here to be 90 kJ/mole) and one half of the energy of formation of the Schottky defects, which in NaCl is $E_S \sim 220$ kJ/mole. Neglecting the

entropy term in Eq (4.21), at 1000 K, $K_S = 3.2\text{x}10^{-12}$ and $C_{VM}^{eq} \sim 1.8\times10^{-6}$. From Eq (5.42) $D_M = 10^{-17}$ cm^2/s.

Ionic solids are rarely so pure that intrinsic point defects control the point defect concentrations. If a divalent impurity cation D is present, the cation vacancy fraction in MX is given by (Problem 5.1):

$$C_{VM} = \frac{1}{2}\left(C_D + \sqrt{C_D^2 + 4K_S}\right) \tag{5.43}$$

where C_D is the site fraction of the divalent cation impurity. This impurity exerts a significant effect on the point defect concentration for C_D as low as $2\text{x}10^{-6}$, for which Eq (5.43) gives $C_{VM} = 3\text{x}10^{-6}$, a 70% increase over C_{VM} in high-purity material. For impurity concentrations greater than a few parts per million, Eq (5.43) reduces to the extrinsic limit, $C_{VM} \sim C_D$. Excepting ultra-high-purity material, the cation diffusivity given by the first of Eq (5.42) in MX is controlled, via C_{VM}, by the concentration of divalent impurity ions. Impurity cations of the same charge, such as K^+, do not affect C_{VM} and hence do not influence the diffusivity of the principal cation.

5.6 Diffusivity measurement methods

The basic transport properties in MX are the self-diffusivities of the two ions, D_M and D_X. Considerable effort has been expended in devising experimental techniques for their measurement.

5.6.1 Surface-tracer method

This method requires that the metal component M has a radioactive isotope, typically an alpha-particle emitter. A thin layer of tracer-enriched MX is deposited on a surface of a single crystal of the same material but of normal isotopic composition.

Figure 5.12 shows how the system operates. Alpha particles emitted at energy E_o lose energy according to the Bragg formula (Ref. 5, Eq (6)). Fortunately, dE/dz is relatively independent of particle energy at these high energies and so can be considered to be a constant in the analysis.

The advantage of the method lies in the ability to collect alpha-energy spectra at different times during an experiment without disturbing the specimen.

The thin layer of MX that is deposited on the single crystal provides M_{tr} moles of the tracer isotope per cm^2 of surface. When heated to a fixed temperature and held for a time t, the tracer self-diffuses into the crystal to produce the volumetric concentration distribution $c_{tr}(z) = C_{tr}(z)/\Omega$ shown in the figure (Ω is the volume of a cation). This is a classic instantaneous plane-source problem for which the solution is (Eq (5.17)):

(5.44)

$$c_{tr} = \frac{M_{tr}}{\sqrt{\pi D_M t}} \exp\left(-\frac{z^2}{4D_M t}\right)$$

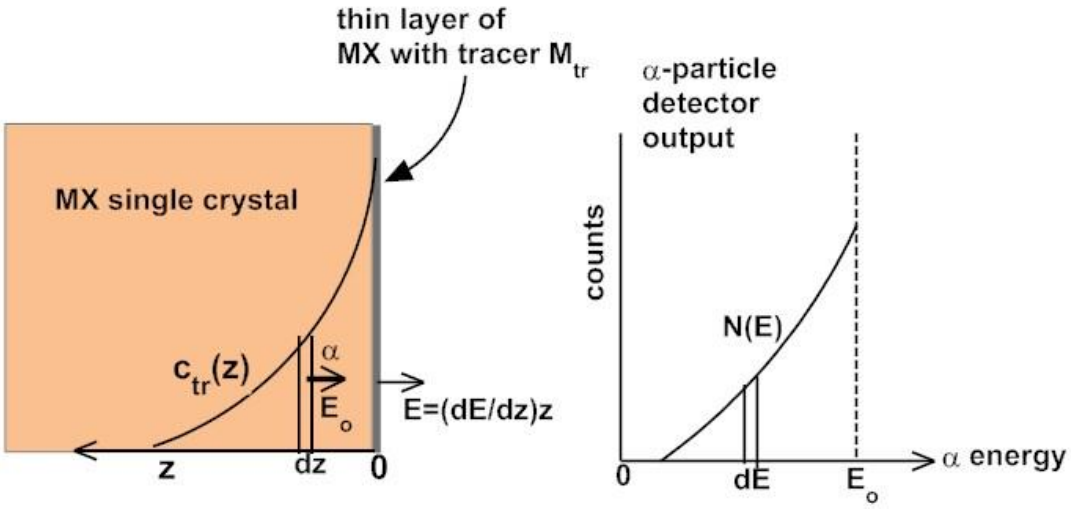

Fig. 5.12 Measurement of cation self-diffusivity in MX using the method of alpha-particle detection

where D_M is the self-diffusion coefficient of M. After a diffusion time t, the slice of the single crystal between z and z+dz emits $\lambda_{tr}c_{tr}(z,t)dz$ alpha particles of energy E_o per second and per cm^2, where λ_{tr} is the decay constant of the tracer. λ_{tr} is small enough that the loss of tracer by radioactive decay over the time interval of the experiment is negligible, which leads to:

(5.45)

$$\int_0^\infty c_{tr}(z,t)dz = M_{tr}$$

Particles directed towards the surface of the crystal leave at energy

$$E = \left(dE/dz\right)_o z \tag{5.46}$$

where $(dE/dz)_o$ is the energy-loss rate at the birth energy. This energy-loss rate is essentially constant over the entire path length z of the alpha particles in the crystal.
At time t, these particles generate *N(E,t)dE* counts in the energy range between E and E + dE. The alpha-emission rate and the count rate are related by:

$$N(E,t)dE = B\lambda_{tr}c_{tr}(z,t)dz \tag{5.47}$$

B is a collection of instrumental constants and the fraction of alpha particles that are emitted in the solid angle subtended by the detector. Integrating Eq (5.47) and using Eq (5.45) gives:

$$B = \frac{\int_0^{E_o} N(E,t)dE}{\lambda_{tr} M_{tr}} \qquad (5.50)$$

In Eq (5.49), B is replaced by Eq (5.50), $c_{tr}(z,t)$ by Eq(5.44) and dE/dz by Eq (5.48). The result is:

$$\frac{\exp(-z^2/4D_{tr}t)}{\sqrt{\pi D_{tr}t}} = \frac{N(E,t)}{\int_0^{E_o} N(E,t)dE}\left(\frac{dE}{dz}\right)_o \qquad (5.48)$$

At a specified diffusion time t, the right-hand side of this equation is a measurable function of E, or, using Eq (5.46), a function of z. This function is fitted to the left-hand side of Eq (5.48) by choosing D_{tr}. This procedure is repeated for several diffusion times, and the resulting best-fit D_{tr} values should be the same (within experimental error).

5.6.2 Diffusion-couple (Boltzmann-Mantano) method

The setup for determining the mutual diffusion coefficient of metals in an alloy or cations in ionic crystals is sketched in Fig. 5.13. It is the analog of the method applied to elemental solids in Sect. 5.3.1. In the top drawing, a block of the mixed-cation crystal (A,B)X is tightly pressed against a block of BX to form a diffusion *couple*. The blocks are sufficiently thick to be treated as semi-infinite media for z < 0 and z > 0. After time t the A-fraction profile $C_A(z,t)$ is shown in the middle drawing. In this example, the site fraction of A, C_A, is the same as the mole fraction x_A.

Both the mutual diffusion coefficient D_{AB} and the specific volume $v = C_A\bar{v}_A + C_B\bar{v}_B$ are functions of composition (C_A). $\bar{v}_A$ and $\bar{v}_B$ are the partial molar volumes of the two components (if the binary solid is ideal, the partial molar volumes are equal to the molar volumes of the pure species). The difference between the molar volumes of A and B is the origin of the marker movement in Kirkendall's experiment (Sect. 5.4), irrespective of the mechanism of diffusion.

The evolution of the A concentration from the initial state to the distribution shown in the middle sketch is governed by the diffusion equation:

$$\frac{\partial C_A}{\partial t} = \frac{\partial}{\partial z}\left(\tilde{D}_{AB}\frac{\partial C_A}{\partial z}\right) \qquad (5.49)$$

The flux of component A (in parentheses) is defined relative to the volume-average velocity (Eq (A-8) in Appendix A).

The initial conditions are:

$$C_A = Y \text{ for } z < 0 \text{ and } C_A = 0 \text{ for } z > 0 \qquad (5.50)$$

$C_A = C_A^o$ for z < 0 and

The boundary conditions for infinitely-thick blocks are

$C_A = C_A^o$ for $z = -\infty$ and

$$C_A = 0 \quad for \; z = \infty \tag{5.51}$$

$$\partial C_A / \partial z = 0 \quad at \quad z = \pm\infty$$

A variable change suitable for this problem is:

$$u = \frac{z}{\sqrt{t}} \quad \text{which gives} \quad \frac{\partial C_A}{\partial t} = -\frac{u}{2t}\frac{dC_A}{du} \quad \text{and} \quad \frac{\partial}{\partial z} = \frac{1}{\sqrt{t}}\frac{d}{du} \tag{5.52}$$

$$\frac{\partial}{\partial z} = \frac{1}{\sqrt{t}}\frac{d}{du}$$

For constant diffusivity, applying Eq (5.52) to Eq (5.49) yields:

(5.56)
(5.53)

$$-\frac{u}{2}\frac{dC_A}{du} = \tilde{D}_{AB}\frac{d^2C_A}{du^2}$$

which is integrated from $C_A = 0$, where $(dC_A/du) = 0$, to any location in the distribution:

(5.57)

$$-\tfrac{1}{2}\int_0^{C_A} u\, dC_A = D_{AB}\frac{dC_A}{du}$$

Replacing u using $u = z/\sqrt{t}$ and $dC_A/du = \sqrt{t}\,dC_A/dz$ yields *Matano's equation*:

$$D_{AB}(C_A) = -\frac{1}{2t}\left(\frac{dz}{dC_A}\right)\int_0^{C_A} z\, dC_A' \tag{5.58}$$

This equation permits the chemical diffusivity to be obtained graphically from the experimental $C_A(z)$ distribution at any time t. In order to use Eq (5.58), the dependent and independent variables are reversed, and the distribution in the bottom diagram of Fig. 5.13 is treated as $z(C_A)$.

The contents of the parentheses in Eq (5.56) is the diffusional flux of A; that is, it is the flux relative to a plane through which the mixture velocity is zero. This plane, called the Montano plane, is located at the origin z = 0. The Mantano plane moves with respect to the fixed plane in Fig. 5.13.

The z = 0 location is obtained by noting that at $z = -\infty$, $C_A = C_A^o$ and $(dC_A/dz) = 0$. This gradient condition in Eq (5.58) requires:

$$\int_0^{C_A^o} z\,dC_A = 0 \qquad (5.59)$$

Equation (5.59) is the area under the $z(C_A)$ curve. The Matano plane is placed so that the area under the $z(C_A)$ curve to the left of the plane equals the area under the curve to the right of the plane. In terms of the notation in the bottom plot of Fig. 5.13, this is $A_L = A_R + A'_R$.

In order to determine D_{AB} at an arbitrary point (say point c in the figure), the bottom plot is turned 90^o so that the curve appears as the $z(C_A)$ distribution. In this orientation, the integral in Eq (5.58) is the area A'_R and the derivative is the tangent to the curve at point c. Accurate methods of determining these quantities are discussed in Ref. [4], p. 35.

Example # 8 - Chemical diffusivity by the Matano method

Find the chemical diffusion coefficient at point c in Fig. 5.13 ($C_A = 0.05$, $z = 2.7$ μm). The anneal time is 5 hours.

The slope of the tangent line is: $dz/dC_A \sim -80$ μm

An approximation to A'_R is a rectangle with point c as one corner and a triangle with the hypotenuse connecting point c with 7.4 μm on the z axis:

$$A'_R = \int_0^{0.05} z\,dC_A = 0.32\ \mu m$$

$$D_{AB}t = \tfrac{1}{2}(80)(0.32)(10^{-4})^2 = 1.3\times10^{-7}\ cm^2$$

For $t = 5\times3600 = 1.8\times10^4$ s, $D_{AB} = 7\times10^{-12}\ cm^2/s$

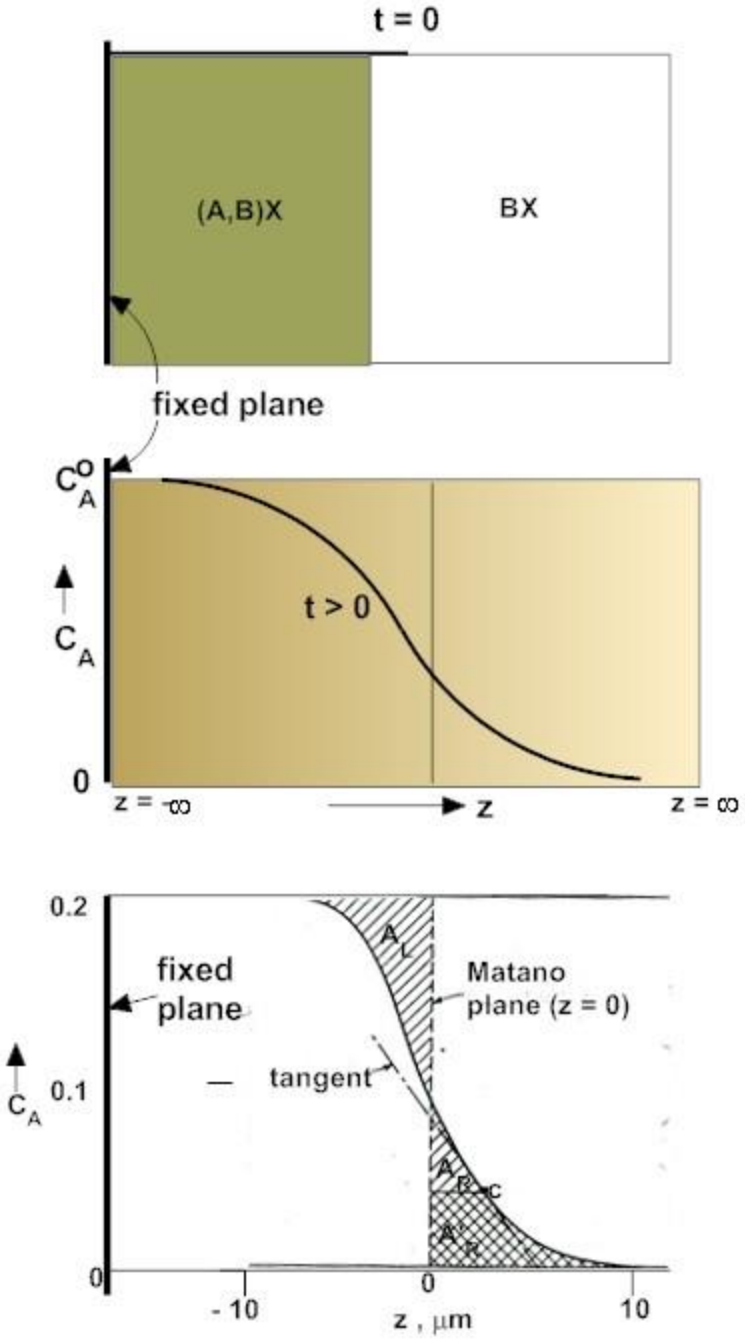

Fig. 5.13 Matano's method of determining a chemical diffusion coefficient (Ref. [4], p.34)

5.7 Diffusion in a thermal gradient (Soret effect)

The Soret effect refers to the transport of atoms driven by a temperature gradient. Unlike ordinary diffusion in a concentration gradient, thermal diffusion is not a random-walk process; the affected atoms flow along the temperature gradient, either up or down, that is, they preferentially move in a particular direction. Diffusion under a temperature gradient acts on impurity atoms in a host crystal, one important example being hydrogen in Zircaloy (Chap. 23).

The Soret effect is characterized by a property of the species in the solid called the *heat of transport*, which is denoted by Q* in units of kJ/mole. Thermal diffusion is accounted for by an additive term to the concentration gradient in the flux equation:

$$J_{imp} = -D\frac{d\,c_{imp}}{dz} - D\frac{Q^* c_{imp}}{RT^2}\frac{dT}{dz} \tag{5.60}$$

A simple method for measuring Q* is available: a rod of the host solid initially containing a uniform concentration of an impurity species is heated to temperature T_L at one end and maintained at a lower temperature T_o at the other end until the equilibrium distribution is reached. The rod is then cut into slices and the concentration of the impurity species c_{imp} measured as a function of z. Because the impurity species cannot leave the rod at either end, it merely redistributes in the rod under the influence of the temperature gradient.

After a time sufficient for steady state to be achieved, the flux is everywhere zero. Setting $J_i = 0$ in Eq (5.60) **Error! Reference source not found.** and eliminating dz results in:

$$d\ln c_{imp} = T_Q\, d\left(\frac{1}{T}\right) \qquad \text{where} \qquad T_Q = \frac{Q^*}{R} \tag{5.61}$$

integrating yields:

$$c_{imp} = B e^{T_Q/T} \tag{5.62}$$

Plotting lnc Vs 1/T yields a straight line whose slope is Q^*/R_g. . The slope, and hence Q*, can be either positive or negative.

Appendix A - Darken's equation

Darken's equation [16]relates the self-diffusion coefficients of the two solutes (D_A, D_B) to the *mutual diffusion coefficient,* also known as the *interdiffusion coefficient,* $\tilde{D}_{AB}$

Before dealing with the diffusion processes, several relationships between two solute components (A and B) in a solution (solid or liquid) are summarized. The principal quantities are:

c_A, c_B = concentrations, moles A,B /vol

x_A, x_B = mole fractions, moles A,B/total moles

$\bar{v}_A, \bar{v}_B$ = partial molar volumes, volume A,B/mole A,B

μ_A, μ_B = chemical potentials of A,B

The total molar volume is:

$$v = x_A\bar{v}_A + x_B\bar{v}_B, \text{ volume/mole} \qquad \text{(A-1)}$$

Relation between mole fraction and concentration:

$$x_A = c_A v \qquad x_B = c_B v \qquad \text{(A-2)}$$

Dividing Eq (A-1) by v and using Eq (A-2):

$$c_A\bar{v}_A + c_B\bar{v}_B = 1 \qquad \text{(A-3)}$$

The chemical potentials are:

$$\mu_A = g_A^o + RT\ln(a_A) \qquad \mu_B = g_B^o + RT\ln(a_B) \qquad \text{(A-4)}$$

where:

g_A^o, g_B^o = Gibbs energies of pure A, B

a_A, a_B = activities of A and B (see Sect. 2.6.5)

R_g = gas constant, 8.314 J/mole-K

T = temperature, K

Dividing the Gibbs-Duhem equation (Eq (2.41)) by v and using Eq (A-2) gives:

$$c_A\nabla\mu_A + c_B\nabla\mu_B = 0 \qquad \text{(A-5)}$$

The fluxes of the components relative to a fixed plane in the medium are the products of their velocities (relative to the same plane) and their concentrations

$$J_A = c_A u_A \qquad J_B = c_B u_B \qquad \text{(A-6)}$$

J_A and J_B are in opposite directions, as are u_A and u_B.

Each component has an intrinsic mobility ω_A, ω_B that is independent of the diffusive flux of the other component. The mobility is the ratio of a velocity to a force. In the present case, the force is the negative of the chemical potential gradient:

$$u_A = -\omega_A\nabla\mu_A \qquad u_B = -\omega_B\nabla\mu_B \qquad \text{(A-7)}$$

The mutual diffusion coefficient of A and B is defined in terms of the *volume-average velocity*:

$$u_V = J_A \bar{v}_A + J_B \bar{v}_B \tag{A-8}$$

This equation can be understood as follows. The product of the flux J_A and the partial molar volume $\bar{v}_A$ is the volume of A transported across a unit area of the fixed plane. Similarly, $J_B \bar{v}_B$ is the velocity of B moving in the opposite direction. The sum in Eq (A-8) is the net volume per unit area moved across the fixed plane or the volume-average velocity u_V.

The mutual diffusion coefficient of A and B is defined in terms of the flux of A through to a plane moving with volume-average velocity:

$$J_A^{u_V} = c_A(u_A - u_V) \equiv -\tilde{D}_{AB} \nabla c_A \tag{A-9}$$

Eliminating u_v in Eq (A-9) using Eq (A-8) and using Eqs (A-3) and the first of Eqs (A-1) changes the first equality of \ Eq (A-9) to:

$$J_A^{u_v} = (J_A c_B - J_B c_A)\bar{v}_B \tag{A-10}$$

u_A and u_B are now eliminated between Eqs (A-6) and (A-7) and the resulting equations for J_A and J_B substituted into Eq (A-10). Then $\nabla \mu_B$ is eliminated by means of Eq (A-5). The result is:

$$J_A^{u_V} = -c_A \bar{v}_B (c_B \omega_A + c_A \omega_B) \nabla \mu_A = -\tilde{D}_{AB} \nabla c_A \tag{A-11}$$

Combining Eqs (A-1) and (A-2), yields:

$$\frac{c_A}{x_A} = \frac{1}{x_A \bar{v}_A + x_B \bar{v}_B}$$

Setting $x_B = 1 - x_A$ in the above, solving for c_A and taking the derivative with respect to x_A yields:

$$\frac{\nabla \ln c_A}{\nabla \ln x_A} = \frac{\bar{v}_B}{x_A \bar{v}_A + x_B \bar{v}_B} \tag{A-12}$$

In Eq (A-12) $\nabla c_A / c_A = \nabla \ln c_A$ and $\nabla x_A / x_A = \nabla \ln x_A$. Multiplying and dividing Eq (A-11) by $\nabla \ln x_A$, then using Eq (A-12) to eliminate by $\nabla \ln c_A / \nabla \ln x_A$ results in:

$$\tilde{D}_{AB} = \frac{\partial \mu_A}{\partial \ln x_A}(x_B \omega_A + x_A \omega_B) \tag{A-13a}$$

Where ∇ has been replaced by ∂. The mobility of species and their *self-diffusion coefficients* (D_A and D_B) are related by the Nernst-Einstein equation:

$$\omega_A = D_A / R_g T \qquad\qquad \omega_B = D_B / R_g T \tag{A-14}$$

Substituting Eq (A-14) into Eq (A-13a) and eliminating chemical potentials using Eq (A-4) yields Darken's equation:

$$\tilde{D}_{AB} = \left[\frac{\partial \ln a_A}{\partial \ln x_A}\right](x_B D_A + x_A D_B) \tag{A-13b}$$

Appendix B Similarity Transformation Solution to Eqs (5.8) – (5.12)

The objective is to convert the Eq (5.5) into an ordinary differential equation which can be solved analytically. To this end, the following dimensionless variables are introduced:

$$\theta = c/c_o \text{ (source)} \tag{B.1a}$$

$$\theta = c/(c_o/2) \quad \text{(couple)} \tag{B.1b}$$

$$\xi = \frac{z}{2\sqrt{D_A t}} \tag{B.2}$$

Equation (B.2) is called the similarity transformation. The new variable ξ is a function of both z and t. In terms of this variable, the partial derivatives in Eq (5.8) are:

$$\frac{\partial c_A}{\partial t} = \frac{\partial \xi}{\partial t}\frac{\partial c_A}{\partial \xi} = \frac{z}{2\sqrt{D_A}}\left(\frac{-1}{2t^{3/2}}\right)\frac{\partial c_A}{\partial \xi} = -\frac{\xi}{2t}\frac{\partial c_A}{\partial \xi}$$

$$\frac{\partial c_A}{\partial z} = \frac{\partial \xi}{\partial z}\frac{\partial c_A}{\partial \xi} = \frac{1}{2\sqrt{D_A t}}\frac{\partial c_A}{\partial \xi}$$

$$\frac{\partial^2 c_A}{\partial z^2} = \frac{\partial}{\partial z}\left(\frac{\partial c_A}{\partial z}\right) = \frac{\partial \xi}{\partial z}\frac{\partial}{\partial \xi}\left(\frac{1}{2\sqrt{D_A t}}\frac{\partial c_A}{\partial \xi}\right) = \frac{1}{4D_A t}\frac{\partial^2 c_A}{\partial \xi^2}$$

Using these transformations in Eq (5.8) converts the partial differential equation to an ordinary differential equation:

$$\frac{d^2\theta}{d\xi^2} + 2\xi\frac{d\theta}{d\xi} = 0 \tag{B.3}$$

The initial and boundary conditions reduce to:

$$\theta = 1 \quad \text{at} \quad \xi = 0 \qquad \text{(Eqs (5.10) and (5.11)} \tag{B.4}$$

$$\theta = 0 \qquad \text{at} \quad \xi = \infty \quad \text{(Eq (5.12)} \tag{B.5}$$

Solution of Eq (B.3) subject to Eqs (B.4) and (B.5) is accomplished by introducing a new dependent variable $U = d\theta/d\xi$, which reduces Eq (B.3) to a first order differential equation:

$$dU/d\xi + 2\xi U = 0$$

The first integral of this equation is:

$$U = \frac{d\theta}{d\xi} = A\exp(-\xi^2)$$

Integrating again:

$$\theta = A\int_0^{\xi}\exp(-\xi'^2)d\xi' + B$$

Applying the boundary conditions given by Eqs (B.4) and (B.5) yields the integration constants:

$$B=1 \quad \text{and} \quad A = -\left\{\int_0^{\infty}\exp(-\xi^2)d\xi\right\}^{-1} = -\frac{2}{\sqrt{\pi}}$$

The dimensionless form of the solution is:

$$\theta = 1 - \frac{2}{\sqrt{\pi}}\int_0^{\xi}\exp(-\xi'^2)d\xi' = 1 - \text{erf}(\xi) = \text{erfc}(\xi) \qquad \text{(B.6)}$$

which, when returned to dimensional forms using Eqs (B.1) and (B.2), yields
Eqs (5.13) and (5.14).

Appendix C Laplace Transform Solution to Eqs (5.21) – (5.23)

The first steps are to introduce dimensionless variables and a new independent variable that converts the diffusion equation from spherical to slab geometry:

$$\eta = r/R_{gr}; \qquad \tau = D_{fg}\, t / R_{gr}^2 \qquad u = \eta c_{fg}/c_{fgo} \tag{C.1}$$

Subscript gr means "grain" and fg signifies "fission-gas".

Substituting Eq (C.1) into Eqs (5.21) - (5.23) yields:

$$\frac{\partial u}{\partial \tau} = \frac{\partial^2 u}{\partial \eta^2} \tag{C.2}$$

$$u(\eta,0) = \eta \tag{C.3}$$

$$u(0,\tau) = 0; \qquad u(1,\tau) = 0 \tag{C.4}$$

Taking the Laplace transform of Eq (C.2) using Eq (C.3)*;

$$\frac{d^2\tilde{u}}{d\eta^2} = p\tilde{u} - \eta \tag{C.5}$$

where p is the transform variable. . The transformed boundary conditions of Eq (C.4)) become:

$$\tilde{u}(0) = \tilde{u}(1) = 0 \tag{C.6}$$

The solution of the transformed equation is:

$$\tilde{u} = -\frac{e^{\sqrt{p}\eta} - e^{-\sqrt{p}\eta}}{p\left(e^{\sqrt{p}} - e^{-\sqrt{p}}\right)} + \frac{\eta}{p} \tag{C.8}$$

Before inverting the solution, the average concentration is first obtained:

$$\frac{\bar{c}_{fg}}{c_{fg\,o}} = \frac{1}{\frac{4}{3}\pi a^3} 4\pi \int_0^a r^2 \frac{c_{fg}(r,t)}{c_{fg\,o}} dr = 3\int_0^1 \eta u d\eta \tag{C.9}$$

* The Laplace transform of the time derivative of a function is the transform variable times the transform of the function minus the initial spatial distribution

Taking the Laplace transform of Eq (C.9) and using Eq (C.8) yields:

$$\frac{\tilde{\bar{c}}_{fg}}{c_{fg_o}} = 3\int_0^1 \eta\,\tilde{u}\,d\eta = \frac{1}{p} - 3\frac{\left(\sqrt{p}-1\right)+\left(\sqrt{p}+1\right)e^{-2\sqrt{p}}}{p^2\left(1-e^{-2\sqrt{p}}\right)} \qquad \text{(C.10)}$$

Short times are equivalent to large values of p, so the terms with $e^{-2\sqrt{p}}$ can be neglected in Eq (C.10), giving:

$$\frac{\tilde{\bar{c}}_{fg}}{c_{fg_o}} = \frac{1}{p} - 3\frac{\sqrt{p}-1}{p^2} = \frac{1}{p} - \frac{3}{p^{3/2}} + \frac{3}{p^2}$$

This transform of the average concentration can be inverted from the table of inverse Laplace transforms to yield :

$$\frac{\bar{c}_{fg}}{c_{fg_o}} = 1 - \frac{6}{\sqrt{\pi}}\sqrt{\tau} + 3\tau \qquad \text{(C.11)}$$

from which Eq (5.24) is obtained

References

1. H. Carslaw & J. Jaeger, "*Conduction of Heat in Solids"*, 2nd Ed., Oxford (1959)
2. J. C. Crank, "*The Mathematics of Diffusion"* Oxford (1964)
3. D. R. Olander, "*Fundamental Aspects of Nuclear Reactor Fuel Elements"*, National technical Information Service, TID-26711-P1 (1976)
4. P. Shewmon, "*Diffusion in Solids"*, 2nd Ed., Minerals, Metals & Materials Society (1989)
5. W. Breitung, "*Oxygen Self- and Chemical Diffusion Coefficients in $UO_{2\pm x}$",* J. Nucl. Mater. **74** (1978) 10
6. Hj. Matzke, "*Atomic Mechanisms of Mass Transport in Ceramic Nuclear Fuel Materials"*, J. Chem. Soc. Faraday Trans. **86** (1990) 1243
7. G. Murch & C. Catlow, *"Oxygen diffusion in UO_2, ThO_2 & PuO_2"*, J. Chem. Soc. Faraday Trans 2 **83** (1987) 1157
8. G. Murch & R. Thorn, *"The mechanism of oxygen diffusion in near-stoichiometric uranium dioxide"*, J. Nucl. Mater. **71** (1977) 219
9. G. Murch, *"Oxygen diffusion in UO_2 – an overview"* Diffusion and Defect Data, **32** (1983) 4
10. Hj. Matzke, *Diffusion in Ceramic Oxide Systems,* Adv. in Ceramics **17** (1986) 1
11. Hj. Matzke, *Diffusion Processes in Nuclear Fuels*, J. Less-Common Metals **121** (1986) 537
12. Hj. Matzke, *"On uranium self-diffusion in UO_2 and UO_{2+x}"* J. Nucl. Mater. **30** (1969) 26
13. D. Glasser-Leme & Hj. Matzke, *"Interdiffusion & chemical diffusion in the UO_2-(U,Pu)O_2 system"* J. Nucl. Mater. 106 (1982) 211; Solid-state Ionics **12** (1984) 217
14. M. Stan & P. Cristea,*"Defects & oxygen diffusion in PuO_{2-x}"*, J. Nucl. Mater. **344** (2005) 213
15. F. Schmitz and R. Lindner, *"Diffusion of heavy elements in nuclear fuel"* J. Nucl. Mater. **17** (1965) 259
16. L. Darken, Trans. Amer. Inst. Mining Metall. Engin. **175** (1948) 184
17. A. R. Cooper and J. H. Heasley, J., Amer. Ceramic Soc. **49** (1966) 280
18. A.D. Smigelskas and E.O. Kirkendall, *"Zinc Diffusion in Alpha Brass*," Trans. AIME, **171** (1947), pp. 130-142.
19. H. Nakajima, Journal of Metals, **49** (6) (1997), pp. 15-19

Problems

5.1 From Eqs (5.33) and (5.34), show why the self-diffusion coefficient varies as $\sqrt{K_{NRT}}$ at low temperature.

(a) Compare D calculated from the method of part (a) with the value from Fig. 5.9 at 800 K and $K_{NRT} = 10^{-6}$ dpa/s.

5.2 Using the Schottky equilibrium constant for MX, derive Eq (5.36).

5.3 Using Eqs (2.42) and (2.43), prove that $\frac{d \ln a_A}{d \ln x_A}$ in Eq (5.1a) can be replaced by $\frac{d \ln a_B}{d \ln x_B}$

5.4 How long is required for a sphere of material A of radius $R_o = 10$ μm to dissolve in an infinite medium of B? The solubility of the sphere material in the matrix is $[A]_o = 10^{-2}$ moles/cm^3. The diffusivity of A in B is $D_{AB} = 10^{-9}$ cm^2/s. The density of solid A is 0.1 moles/cm^3.
Even though the sphere is shrinking, assume steady-state diffusion.

5.5. The diffusion of element A into element B is described by Eq (5.13). At the temperature the experiment is conducted of 400 K the diffusion coefficient of A into B is equal to 10^{-11} cm^2/s.
If C_o=1 (such as would occur when there is an inexhaustible supply of A at x=0),.

a) After 2 days of running the experiment, at what distances into the sample would the concentrations be equal to 0.5 and to 0.1?
b) For a distance of 1 cm, at what time would you expect to see a concentration of 0.1?
c) How would the answers to the above questions change if the absolute temperature was twice the value of the initial temperature? Assume the activation energy for migration of A into B is 1 eV, and that all other terms of Einstein's diffusion coefficient formula are independent of temperature.6

5.6. Given that you are able to perform a diffusion experiment during a period of 30 days and that you are able to analyze a diffusion layer with thickness of order of 10^{-3}cm, what is a rough estimate of the smallest diffusion coefficient that could be studied? If the

sample is Cu, what is the lowest temperature at which the experiment could be made? If the temperature is increased to 950°C, how does this affect the time needed to achieve the same result? (Given that for Cu, $D_o = 0.6\, cm^2 s^{-1}$; $Q(\text{activation energy}) = 1.85\,\text{eV/atom}$)

5.7. It is desired to create a 0.2 mm carburized layer in a steel component by diffusing carbon into it through exposure to a carburizing gas at high temperature for a time t. The diffusion coefficient of C into fcc Fe at 1000 C is 4 x 10^{-11} m^2s^{-1}. The surface concentration of carbon is 0.5.

a) Use the Einstein formula to find the activation energy. Assume $\nu = 10^{13}$ Hz and a jump distance of 2.04 x 10^{-10} m.

b) Use the solution for the concentration profile established in a diffusion couple, to derive the annealing time necessary to obtain a 1 at % concentration of C over the desired thickness.

5.8 Using Appendix A, show how the volume-average velocity u_V can be obtained from the curve of c_A vs z. The A-B solution is ideal.

5.9 (a) At 800 K, how long is required for a vacancy to undergo 100 diffusive jumps? (see Example #5). The vacancy migration energy is 1.0 eV.

(b) In the same time interval, how many jumps does a self-interstitial atom (SIA) make? The SIA migration energy is 0.7 eV.

5.10 The sketch below shows a recombination event in two dimensions. Figure 10 is the 3D version.

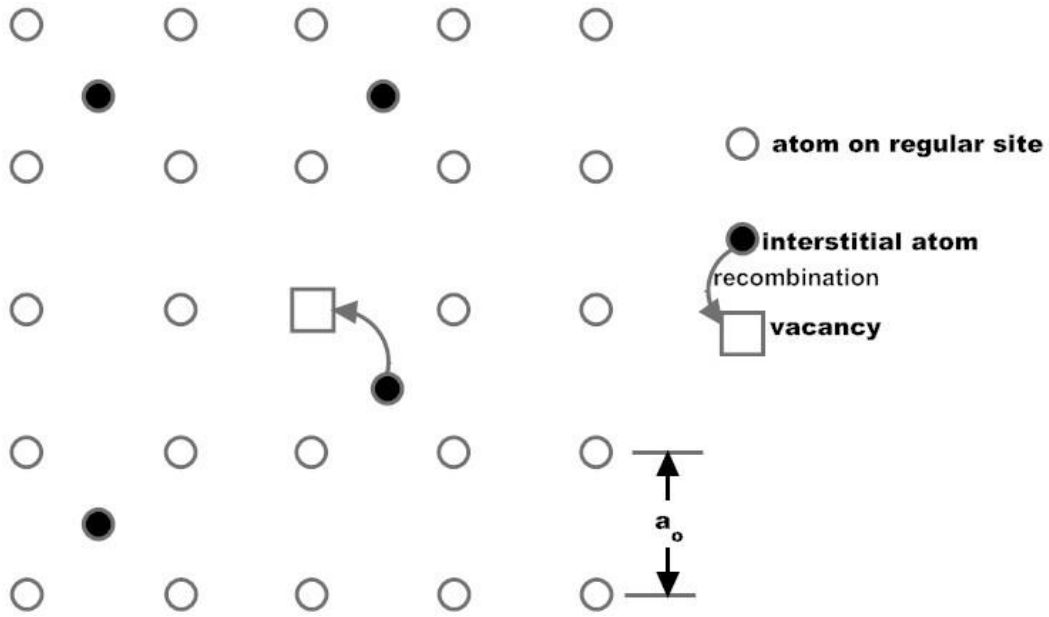

The rate of vacancy-interstitial recombination rate is:

$$R_R = \alpha D_I c_I c_V \text{ recombinations/unit area -s.}$$

The vacancy diffusion coefficient is very small compared to D_I for interstitials. c_I and c_V are the areal concentrations (i.e. number per unit area).

(a) What is the Einstein relation in 2D?
(b) What is the numerical value of □ in the recombination rate equation?

5.11. In a solid state diffusion experiment to measure diffusion coefficients, a layer of radioactive gold atoms (denoted Au*) is deposited onto a block of non-radioactive fcc gold.

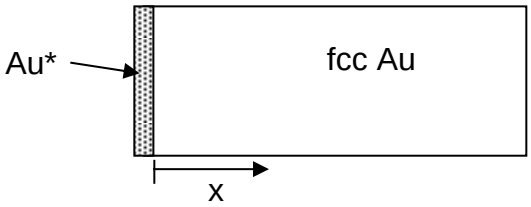

(a) Explain briefly how the experiment would be conducted to determine the diffusion coefficient

b) During the experiment the activation energy (migration plus formation) for diffusion in this material is determined to be Q=1.67 eV. Given that diffusion occurs by a vacancy mechanism, calculate the diffusion coefficient in Au at 1070 K. The lattice parameter for fcc gold is a_o= 0.408 nm and the vibration frequency is 5 x 10^{12} Hz.

c) Using the diffusion coefficient above, calculate the concentration of radioactive gold at x=20 microns after one week. How long would one have to wait to obtain a concentration of 50% radioactive gold at that distance? Consider that the concentration of radioactive gold at x=0 is 100% throughout the experiment.